# SPECTROSCOPIC DIAGNOSTICS OF OVERSTRESSED NANOSECOND DISCHARGE PLASMA BETWEEN ZINC ELECTRODES IN AIR AND NITROGEN

O. K. Shuaibov, R. V. Hrytsak, O. I. Minya, A. A. Malinina, Yu. Yu. Bilak, Z. T. Gomoki
*Uzhhorod National University,*
*3, Narodna Sq., Uzhhorod, UA–88000, Ukraine*

(Received 11 January 2022; in final form 05 April 2022; accepted 07 April 2022; published online 27 May 2022)

The paper presents emission spectra of an overstressed nanosecond discharge between zinc electrodes in air and nitrogen at pressures of 13.3 kPa and 20 kPa, respectively. In the process of microexplosions of inhomogeneities on the working surfaces of zinc electrodes in a strong electric field, zinc vapor is introduced into the discharge gap during the formation of ectons. This creates prerequisites for the formation of molecules and clusters of zinc, oxide and zinc nitride in plasma and the synthesis of thin nanostructured films of zinc, oxide and zinc nitride, which can be deposited on a glass or quartz substrate installed near the center of the discharge gap.

The spectral characteristics of the discharge were investigated from the central part of the discharge gap 2 mm in size. The main excited components of the plasma of vapor–gas mixtures based on zinc vapor and air and nitrogen have been identified, which, when deposited outside the discharge plasma, can lead to the formation of thin nanostructured films of zinc, nitride and zinc oxide.

**Key words:** overstressed nanosecond discharge, zinc, air, plasma.

DOI: https://doi.org/10.30970/jps.26.2501

## I. INTRODUCTION

A decrease in the distance to 0.5–2.0 mm between metal electrodes in a discharge of nanosecond duration leads to intensive sputtering of the electrode material and the appearance of spectral lines of atoms and ions of copper, iron and zinc in the plasma radiation spectra [1]. When operating in the mode of overvoltage of the interelectrode gap, runaway electrons (electrons that enter the mode of continuous acceleration at high electric field strength) with energies of tens of kilovolts are recorded in the plasma [2]. A spatially uniform discharge is formed in discharge gaps with an inhomogeneous distribution of the electric field strength under the action of a beam of runaway electrons and the accompanying X-ray radiation, which play the role of overionization, which can be used to develop UV lamps with a small volume of the plasma medium ($V < 10$ mm$^3$) [3]. The plasma of such a discharge between copper or zinc electrodes is not only a source of bactericidal UV radiation, but also a flow of copper or zinc oxide nanoparticles [4], which have strong antibacterial properties [5].

The introduction of vapors of the electrode material into the discharge occurs during the formation of ectons (electron avalanche) as a result of microexplosions of inhomogeneities on the surface of metal electrodes, which leads to the appearance of vapors of the electrode material of the surface of the electrodes [6]. A beam of runaway electrons and the accompanying X-ray radiation under these conditions overionize of the discharge gap; therefore, in such discharge systems with an inhomogeneous distribution of the electric field, a homogeneous discharge of a small volume is formed [7]. In particular, in [7], the results of an experimental study of a diffuse nanosecond discharge in nitrogen ($p = 12 - 400$ kPa) in the "cone–plane" gap are presented. At a nitrogen pressure of up to 200 kPa, a large-diameter streamer was formed in the discharge gap.

Such discharges are promising for applications in spectroscopy, medicine, and photobiology. As automatic UV illumination, such sources are promising for use in nanotechnology (in particular, the synthesis of film nanostructures of transition metal oxides in the field of intense UV radiation [8]).

An overvoltage nanosecond discharge in nitrogen and air also occurs in the metal vapors of the electrodes; therefore, film nanostructures based on transition metals and their nitrides and oxides can be synthesized here, which can be deposited on a dielectric substrate located near the electrode system [9]. To optimize the synthesis of film nanostructures based on zinc, zinc oxide and zinc nitride, we study the emission properties of an overvoltage nanosecond discharge between zinc electrodes in nitrogen and air. Such information will make it possible to determine the time-averaged temperature of electrons and their density in the plasma, which was formed in the middle of the discharge gap.

The article presents the results of a spectroscopic study of plasma radiation of an overvoltage nanosecond discharge between zinc electrodes in nitrogen and air, which can be used both as UV bactericidal radiation and for the synthesis of film nanostructures of zinc, nitride and zinc oxide upon automatic irradiation of the substrate with bactericidal UV plasma radiation.

## II. EXPERIMENTAL METHODS AND TECHNIQUE

The study of the characteristics of an overvoltage nanosecond discharge in air and nitrogen was carried out using a dielectric chamber shown in Fig. 1. The discharge between the zinc electrodes was ignited in a sealed Plexiglas chamber. The distance between the electrodes was

$d = 2$ mm. A more detailed diagram of the discharge device and the experimental technique are given in more detail in the works [1,9].

To ignite the discharge, bipolar high-voltage pulses with a duration of 50–150 ns and an amplitude of $\pm(20-40)$ kV were applied to the electrodes of the discharge chamber. The voltage pulse repetition rate was selected in the range of 80–150 Hz.

The discharge gap was overstressed, which created favorable conditions for the formation of a high-energy "runaway" electron beam and accompanying X-ray radiation [2].

Plasma radiation, recorded in the spectral range $\lambda = 196-663$ nm, entered the entrance slit of a spectrometer with a diffraction grating of 1200 lines/mm. An FEP-106 photomultiplier tube connected to a dc amplifier was used at the output of the spectrometer to detect radiation. The signal from the amplifier was fed to an analog-to-digital converter and then fed to a personal computer for processing.

The discharge chamber was evacuated with a foreline pump to a residual pressure of 10 Pa, and then air or nitrogen was fed into the chamber to a pressure of 10–20 kPa. The diameter of the zinc cylindrical electrodes was 5 mm, and the radius of curvature of their working end surface was the same and equal to 3 mm. The discharge volume depended on the voltage pulse repetition rate. The "point discharge" mode was achieved only at voltage pulse repetition rates in the range $f = 40-150$ Hz.

Oscillograms of voltage pulses across the discharge gap and oscillograms of current pulses were recorded using a broadband low-inductance capacitive voltage divider, a Rogowski coil, and a 6LOR-04 broadband oscilloscope. The time resolution of this system for measuring the characteristics of electrical impulses was 2–3 ns. The pulsed electrical power of the overvoltage nanosecond discharge was determined by graphical multiplication of the oscillograms of the voltage and current pulses. Time integration of the pulsed power made it possible to obtain energy in a single electrical pulse introduced into the plasma.

## III. RESULTS AND DISCUSSION

Electrical properties. At an air or nitrogen pressure of 10–20 kPa and $d = 2$ mm, the overstressed nanosecond discharge had the form of a bright central part with a diameter of about $2-3$ mm and a series of weaker plasma jets escaping from its central part. The main reasons for the appearance of the diffuse glow of the discharge between the electrodes can be beams of "runaway electrons" and the accompanying X-ray radiation [2].

Oscillograms of voltage, current and pulsed power for an overvoltage nanosecond discharge between zinc electrodes at an air pressure of 20 kPa and nitrogen of $-13.3$ kPa looked the same as in a similar discharge in air between zinc or copper electrodes [1, 9].

Oscillograms of voltage and current were in the form of oscillations decaying in time with a duration of about 7–10 ns, which is due to the mismatch between the output resistance of the high-voltage modulator and the load resistance. The total duration of the voltage oscillations across the gap and the discharge current reached 400–450 ns with the duration of individual voltage oscillations 7–10 ns, and the current oscillations had a duration of $\approx 70$ ns. For the investigated discharge, the amplitude of the largest voltage drop at the electrodes was achieved at the initial stage of the discharge and was $\approx 7-8$ kV, and the current was 140–160 A. The magnitude of the pulse discharge power reached (0.5–0.7) MW, which ensured the energy contribution to the plasma in one discharge pulse at a level of 30–40 mJ.

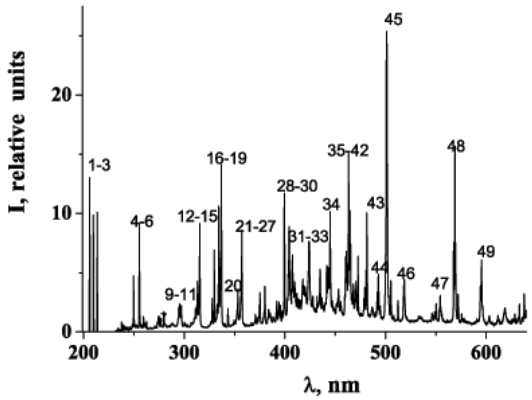


Fig. 1. The emission spectrum of the overvoltage nanosecond discharge in the gas–vapor mixture "air–zinc" at air pressure 13.3 kPa.

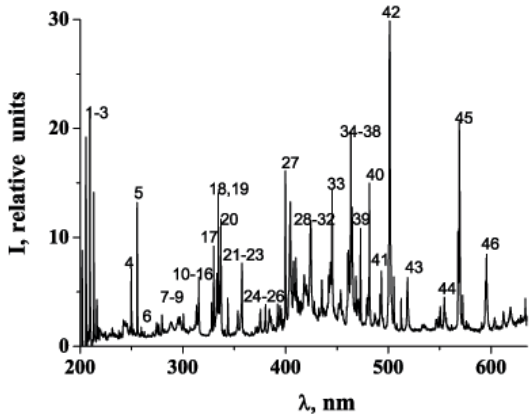


Fig. 2. The spectrum of radiation of the overvoltage nanosecond discharge in the gas–vapor mixture "nitrogen–zinc" at $p(N_2) = 20$ kPa.

The emission spectra of an overvoltage nanosecond discharge in gas–vapor mixtures based on air and nitrogen with zinc are shown in Figs. 1 and 2, and the results of the interpretation of the spectral lines and bands are summarized in Table 1. When decoding the plasma emission spectra, reference books [10, 11] were used.

| No. | $\lambda_{\text{table}}$, nm | $I$, r. u. | Object | $E_{\text{low.}}$, eV | $E_{\text{up.}}$, eV | Lower term | Upper term |
|---|---|---|---|---|---|---|---|
| 1 | 206.20 | 12.76 | Zn II | 0 | 6.01 | $3d^{10}4s$ $^2S_{1/2}$ | $3d^{10}4p$ $^2P^0_{1/2}$ |
| 2 | 209.99 | 9.84 | Zn II | 6.11 | 12.02 | $3d^{10}4p$ $^2P^0_{3/2}$ | $3d^{10}4d$ $^2D_{5/2}$ |
| 3 | 213.85 | 9.06 | Zn I | 0 | 5.79 | $3d^{10}4s^2$ $^1S_0$ | $3d^{10}4s4p$ $^2P^0_1$ |
| 4 | 250.19 | 4.72 | Zn I | 6.01 | 10.96 | $3d^{10}4p$ $^2P^0_{1/2}$ | $3d^{10}5s$ $^2S_{1/2}$ |
| 5 | 255.79 | 8.49 | Zn II | 6.11 | 10.96 | $3d^{10}4p$ $^2P^0_{3/2}$ | $3d^{10}5s$ $^2S_{1/2}$ |
| 6 | 258.24 | 1.32 | Zn I | 4.02 | 8.82 | $3d^{10}4s4p$ $^3P^0_1$ | $3d^{10}4s6d$ $^3D_2$ |
| 7 | 267.05 | 0.32 | Zn I | 4.00 | 8.64 | $3d^{10}4s4p$ $^3P^0_0$ | $3d^{10}4s7s$ $^3S_1$ |
| 8 | 279.92 | 1.74 | N II | 21.60 | 26.03 | 3p $^1D$ | 4d $^1D^0$ |
| 9 | 295.32 | 1.96 | $N_2$ | Second positive system $C^3\Pi^+_u - B^3\Pi^+_g$ (4;2) | | | |
| 10 | 296.20 | 2.45 | $N_2$ | Second positive system $C^3\Pi^+_u - B^3\Pi^+_g$ (3;1) | | | |
| 11 | 297.68 | 2.21 | $N_2$ | Second positive system $C^3\Pi^+_u - B^3\Pi^+_g$ (2;0) | | | |
| 12 | 307.206 | 0.80 | Zn I | 4.07 | 8.11 | $3d^{10}4s4p$ $^3P^0_2$ | $3d^{10}4s6s$ $^3S_1$ |
| 13 | 311.67 | 2 | $N_2$ | Second positive system $C^3\Pi^+_u - B^3\Pi^+_g$ (3;2) | | | |
| 14 | 313.60 | 4.37 | $N_2$ | Second positive system $C^3\Pi^+_u - B^3\Pi^+_g$ (2;1) | | | |
| 15 | 315.93 | 8.78 | $N_2$ | Second positive system $C^3\Pi^+_u - B^3\Pi^+_g$ (1;0) | | | |
| 16 | 328.23 | 2.70 | Zn I | 4.00 | 7.78 | $3d^{10}4s4p$ $^3P^0_0$ | $3d^{10}4s4d$ $^3D_1$ |
| 17 | 330.25 | 6.82 | Zn I | 4.02 | 7.78 | $3d^{10}4s4p$ $^3P^0_1$ | $3d^{10}4s4d$ $^3D_2$ |
| 18 | 334.50 | 10.68 | Zn I | 4.07 | 7.78 | $3d^{10}4s4p$ $^3P^0_2$ | $3d^{10}4s4d$ $^3D_3$ |
| 19 | 337.13 | 14.10 | $N_2$ | Second positive system $C^3\Pi^+_u - B^3\Pi^+_g$ (0;0) | | | |
| 20 | 343.71 | 1.67 | N II | 18.50 | 22.10 | 3s $^1P_0$ | 3p $^1S$ |
| 21 | 353.67 | 3.57 | $N_2$ | Second positive system $C^3\Pi^+_u - B^3\Pi^+_g$ (1;2) | | | |
| 22 | 357.69 | 8.53 | $N_2$ | Second positive system $C^3\Pi^+_u - B^3\Pi^+_g$ (0;1) | | | |
| 23 | 371.05 | 1.51 | $N_2$ | Second positive system $C^3\Pi^+_u - B^3\Pi^+_g$ (2;4) | | | |
| 24 | 375.54 | 3.32 | $N_2$ | Second positive system $C^3\Pi^+_u - B^3\Pi^+_g$ (1;3) | | | |
| 25 | 380.49 | 3.88 | $N_2$ | Second positive system $C^3\Pi^+_u - B^3\Pi^+_g$ (0;2) | | | |
| 26 | 394.30 | 2.42 | $N_2$ | Second positive system $C^3\Pi^+_u - B^3\Pi^+_g$ (2;5) | | | |
| 27 | 399.49 | 11.83 | N II | 18.50 | 21.60 | 3s $^1P_0$ | 3p $^1D$ |
| 28 | 404.13 | 8.83 | N II | 23.14 | 26.21 | 3d $^3F_0$ | 4f G(4 1/2) |
| 29 | 407.58 | 6.39 | O II | 25.65 | 28.69 | 3p $^4D^0_{5/2}$ | 3d $^4F_{7/2}$ |
| 30 | 417.61 | 4.46 | N II | 23.19 | 26.16 | 3d $^1D^0$ | 4f F(2 1/2) |
| 31 | 424.17 | 7.36 | N II | 23.24<br>23.24 | 26.17<br>26.16 | 3d $^3D^0$<br>3d $^3D^0$ | 4f F(3 1/2)<br>4f F(2 1/2) |
| 32 | 434.94 | 5.08 | O II | 23.00 | 25.85 | 3s $^4P_{5/2}$ | 3p $^4P^0_{5/2}$ |
| 33 | 443.27 | 5.51 | N II | 23.41 | 26.21 | 3d $^3P^0$ | 4f D(2 1/2) |
| 34 | 444.70 | 10.06 | N II | 20.41 | 23.19 | 3p $^3D$ | 3d $^3D^0$ |

| № | $\lambda_{\text{table}}$, nm | $I$, r. u. | Object | $E_{\text{low.}}$, eV | $E_{\text{up.}}$, eV | Lower term | Upper term |
|---|---|---|---|---|---|---|---|
| 35 | 460.71 | 6.88 | N II | 18.46 | 21.15 | 3s $^3P^0$ | 3p $^3P$ |
| 36 | 461.38 | 5 | N II | 18.46 | 21.15 | 3s $^3P^0$ | 3p $^3P$ |
| 37 | 462.13 | 14.53 | N II | 18.46 | 21.15 | 3s $^3P^0$ | 3p $^3P$ |
| 38 | 463.05 | 15.18 | N II | 18.47 | 21.15 | 3s $^3P^0$ | 3p $^3P$ |
| 39 | 464.30 | 10.17 | N II | 18.47 | 21.15 | 3s $^3P^0$ | 3p $^3P$ |
| 40 | 468.22 | 4.01 | Ar II | 18.49 | 21.13 | 3d $^2F_{7/2}$ | $4p'$ $^2F^0_{7/2}$ |
| 41 | 470.53 | 4.23 | O II | 26.25 | 28.88 | 3p $^2D^0_{5/2}$ | 3d $^2F_{7/2}$ |
| 42 | 472.21 | 6.43 | Zn I | 4.02 | 6.65 | $3d^{10}4s4p$ $^3P^0_1$ | $3d^{10}4s5s$ $^3S_1$ |
| 43 | 472.21 | 6.43 | Zn I | 4.02 | 6.65 | $3d^{10}4s4p$ $^3P^0_2$ | $3d^{10}4s5s$ $^3S_1$ |
| 44 | 492.40 | 4.87 | Zn II | 12.02 | 14.53 | $3d^{10}4d$ $^2D_{5/2}$ | $3d^{10}4f$ $^2F^0_{7/2}$ |
| 45 | 500.52 | 25.40 | N II | 25.50<br>20.66 | 27.97<br>24.14 | 3s $^5P$<br>3p $^3D$ | 3p $^5P^0$<br>$3d^3F^0$ |
| 46 | 518.62 | 4.36 | N II | 27.98 | 30.36 | 3p $^5P^0$ | 3d $^5D$ |
| 47 | 554.51 | 3.09 | N I | 11.76 | 14.00 | 3p $^4D^0$ | 5d $^4P$ |
| 48 | 567.60 | 14.82 | N II | 18.46 | 20.64 | 3s $^3P^0$ | 3s $^3D$ |
| 49 | 595.42 | 6 | N II | 23.57 | 25.58 | 3d $^1P^0$ | 4p $^1S$ |

Table 1. Results of the identification of the spectrum shown in Fig. 1

Plasma emission spectra based on air, nitrogen and zinc vapor included the emission of atoms and singly charged ions of zinc and nitrogen (Zn I, Zn II, N I and N II), spectral bands of the second positive system of the nitrogen molecule $N_2(C^3\Pi_u^+ - B_3\Pi_g^+)$ and continuous emission (continuum) in the spectral region 210–640 nm. Spectral lines and bands were observed against the background of continuous plasma radiation. The most pronounced continuum in the discharge radiation was observed in the spectral range 400–500 nm. A similar continuum was observed in the radiation of an overvoltage nanosecond discharge between zinc electrodes in air at the atmospheric pressure and was identified with the radiation of zinc oxide nanoparticles [9]. We used nitrogen of "technical" purity, in which the main impurity was oxygen at the level of 0.5–1.0 %; therefore, the formation of zinc oxide nanoparticles was possible in the nitrogen which was used in the experiments.

The spectral lines of zinc atoms and ions were most pronounced in the spectral ranges: (206–268), (307–335), (472–493) nm. The radiation of nitrogen molecules was concentrated in the spectral range (282–394) nm, and the radiation of atomic singly charged nitrogen ions was most manifested in the spectral ranges: (280–344), (400–465) and (500–596) nm.

The distribution of the intensity of the spectral lines of the zinc atom and ion from an overstressed nanosecond discharge in gas–vapor mixtures "air (nitrogen)–zinc" correlated with the distribution of the intensity of spectral lines for a zinc vapor lamp [12].

The intensity of the resonance spectral lines of an atom ($\lambda = 213.85$ nm) and a singly charged zinc ion ($\lambda = 206.20$ nm) in an overstressed nanosecond discharge on the gas–vapor mixture "air–zinc" increased upon going to the mixture of "nitrogen–zinc" for other spectral lines Zn I, Zn II from the spectral range $\Delta\lambda = (206-268)$ nm. The intensity ratio of spectral lines Zn I ($\lambda = 307.21$; $\lambda = 334.50$ nm) in plasma on mixtures based on nitrogen and air with zinc vapor was 2 , 9 and 1.7, respectively. The intensity of the spectral lines with $\lambda = 481.05$ nm Zn I and $\lambda = 492.40$ nm Zn II also increased about two times when passing from a discharge in a mixture based on air to a discharge in a mixture based on nitrogen. Zn I and Zn II lines can be caused by the quenching of their upper excited levels by oxygen molecules, which can lead to the formation of zinc oxide molecules and clusters, which are subsequently transformed into the corresponding nanoparticles.

The intensity of the band with $\lambda = 337.13$ nm $N_2(C^3\Pi_u^+ - B_3\Pi_g^+)$ (0; 0) decreased about 1.5 times. This is due to a decrease in the temperature of electrons in a plasma with a higher concentration of nitrogen molecules, since when nitrogen is excited in nanosecond discharges, the main mechanism is direct electron impact.

The intensity of the spectral line with $\lambda = 500.52$ nm of N II was higher in a discharge in a gas–vapor mixture "nitrogen–zinc" by about 1.2 times in comparison with a plasma based on a mixture "air–zinc".

| No. | $\lambda_{\text{table}}$, nm | $I$, r. u. | Object | $E_{\text{low.}}$, eV | $E_{\text{up.}}$, eV | Lower term | Upper term |
|---|---|---|---|---|---|---|---|
| 1 | 206.20 | 26.23 | Zn II | 0 | 6.01 | $3d^{10}4s$ $^2S_{1/2}$ | $3d^{10}4p$ $^2P^0_{1/2}$ |
| 2 | 209.99 | 31.35 | Zn II | 6.11 | 12.02 | $3d^{10}4p$ $^2P^0_{3/2}$ | $3d^{10}4d$ $^2D_{5/2}$ |
| 3 | 213.85 | 19.28 | Zn I | 0 | 5.79 | $3d^{10}4s^2$ $^1S_0$ | $3d^{10}4s4p$ $^2P^0_1$ |
| 4 | 250.19 | 10.08 | Zn I | 6.01 | 10.96 | $3d^{10}4p$ $^2P^0_{1/2}$ | $3d^{10}5s$ $^2S_{1/2}$ |
| 5 | 255.79 | 19.80 | Zn II | 6.11 | 10.96 | $3d^{10}4p$ $^2P^0_{3/2}$ | $3d^{10}5s$ $^2S_{1/2}$ |
| 6 | 258.24 | 1.88 | Zn I | 4.02 | 8.82 | $3d^{10}4s4p$ $^3P^0_1$ | $3d^{10}4s6d$ $^3D_2$ |
| 7 | 267.05 | 1.2 | Zn I | 4.00 | 8.64 | $3d^{10}4s4p$ $^3P^0_0$ | $3d^{10}4s7s$ $^3S_1$ |
| 8 | 279.92 | 4.06 | N II | 21.60 | 26.03 | $3p\ ^1D$ | $4d\ ^1D^0$ |
| 9 | 281.98 | 2.06 | $N_2$ | Second positive system $C^3\Pi^+_u - B^3\Pi^+_g$ (3;0) | | | |
| 10 | 295.32 | 2.78 | $N_2$ | Second positive system $C^3\Pi^+_u - B^3\Pi^+_g$ (4;2) | | | |
| 11 | 296.20 | 3.11 | $N_2$ | Second positive system $C^3\Pi^+_u - B^3\Pi^+_g$ (3;1) | | | |
| 12 | 297.68 | 3 | $N_2$ | Second positive system $C^3\Pi^+_u - B^3\Pi^+_g$ (2;0) | | | |
| 13 | 307.21 | 2.31 | Zn I | 4.07 | 8.11 | $3d^{10}4s4p$ $^3P^0_2$ | $3d^{10}4s6s$ $^3S_1$ |
| 14 | 311.67 | 2.29 | $N_2$ | Second positive system $C^3\Pi^+_u - B^3\Pi^+_g$ (3;2) | | | |
| 15 | 313.60 | 3.71 | $N_2$ | Second positive system $C^3\Pi^+_u - B^3\Pi^+_g$ (2;1) | | | |
| 16 | 315.93 | 5.26 | $N_2$ | Second positive system $C^3\Pi^+_u - B^3\Pi^+_g$ (1;0) | | | |
| 17 | 328.23 | 6.5 | Zn I | 4.00 | 7.78 | $3d^{10}4s4p$ $^3P^0_0$ | $3d^{10}4s4d$ $^3D_1$ |
| 18 | 330.25 | 13.29 | Zn I | 4.02 | 7.78 | $3d^{10}4s4p$ $^3P^0_1$ | $3d^{10}4s4d$ $^3D_2$ |
| 19 | 334.50 | 18.04 | Zn I | 4.07 | 7.78 | $3d^{10}4s4p$ $^3P^0_2$ | $3d^{10}4s4d$ $^3D_3$ |
| 20 | 337.13 | 9.12 | $N_2$ | Second positive system $C^3\Pi^+_u - B^3\Pi^+_g$ (0;0) | | | |
| 21 | 343.71 | 5.93 | N II | 18.50 | 22.10 | 3s $^1P_0$ | 3p $^1S$ |
| 22 | 357.69 | 6.34 | $N_2$ | Second positive system $C^3\Pi^+_u - B^3\Pi^+_g$ (0;1) | | | |
| 23 | 371.05 | 2.00 | $N_2$ | Second positive system $C^3\Pi^+_u - B^3\Pi^+_g$ (2;4) | | | |
| 24 | 375.54 | 3.48 | $N_2$ | Second positive system $C^3\Pi^+_u - B^3\Pi^+_g$ (1;3) | | | |
| 25 | 380.49 | 3.48 | $N_2$ | Second positive system $C^3\Pi^+_u - B^3\Pi^+_g$ (0;2) | | | |
| 26 | 394.30 | 4.61 | $N_2$ | Second positive system $C^3\Pi^+_u - B^3\Pi^+_g$ (2;5) | | | |
| 27 | 399.49 | 16.41 | N II | 18.50 | 21.60 | 3s $^1P_0$ | 3p $^1D$ |
| 28 | 404.13 | 16.33 | N II | 23.14 | 26.21 | 3d $^3F_0$ | 4f $D$(4 1/2) |
| 29 | 417.61 | 8.74 | N II | 23.19 | 26.16 | 3d $^1D^0$ | 4f $F$(2 1/2) |
| 30 | 424.17 | 13.80 | N II | 23.24<br>23.24 | 26.17<br>26.16 | 3d $^3D^0$<br>3d $^3D^0$ | 4f $F$(3 1/2)<br>4f $F$(2 1/2) |
| 31 | 435.50 | 7.5 | $N_2$ | Second positive system $C^3\Pi^+_u - B^3\Pi^+_g$ (4;9) | | | |
| 32 | 443.27 | 10 | N II | 23.41 | 26.21 | 3d $^3P^0$ | 4f $D$(2 1/2) |
| 33 | 444.70 | 17.95 | N II | 20.41 | 23.19 | 3p $^3D$ | 3d $^3D^0$ |
| 34 | 460.71 | 10.45 | N II | 18.46 | 21.15 | 3s $^3P^0$ | 3p $^3P$ |
| 35 | 461.38 | 10.39 | N II | 18.46 | 21.15 | 3s $^3P^0$ | 3p $^3P$ |

| № | $\lambda_{\text{table}}$, nm | $I$, r. u. | Object | $E_{\text{low.}}$, eV | $E_{\text{up.}}$, eV | Lower term | Upper term |
|---|---|---|---|---|---|---|---|
| 36 | 462.13 | 9.85 | N II | 18.46 | 21.15 | 3s $^3P^0$ | 3p $^3P$ |
| 37 | 463.05 | 23.55 | N II | 18.47 | 21.15 | 3s $^3P^0$ | 3p $^3P$ |
| 38 | 464.30 | 23.47 | N II | 18.47 | 21.15 | 3s $^3P^0$ | 3p $^3P$ |
| 39 | 472.21 | 12.71 | Zn I | 4.02 | 6.65 | $3d^{10}4s4p$ $^3P_1^0$ | $3d^{10}4s5s$ $^3S_1$ |
| 40 | 481.05 | 19.85 | Zn I | 4.07 | 6.65 | $3d^{10}4s4p$ $^3P_2^0$ | $3d^{10}4s5s$ $^3S_1$ |
| 41 | 492.40 | 10.98 | Zn II | 12.02 | 14.53 | $3d^{10}4d$ $^2D_{5/2}$ | $3d^{10}4f$ $^2F^0_{7/2}$ |
| 42 | 500.52 | 31.06 | N II | 25.50<br>20.66 | 27.97<br>24.14 | 3s $^5P$<br>3p $^3D$ | 3p $^5P^0$<br>3d $^3F^0$ |
| 43 | 518.62 | 8.36 | N II | 27.98 | 30.36 | 3p $^5P^0$ | 3d $^5D$ |
| 44 | 554.51 | 6.56 | N I | 11.76 | 14.00 | 3p $^4D^0$ | 5d $^4P$ |
| 45 | 567.60 | 28.17 | N II | 18.46 | 20.64 | 3s $^3P^0$ | 3p $^3D$ |
| 46 | 595.42 | 11.71 | N II | 23.57 | 25.58 | 3d $^1P^0$ | 4p $^1S$ |

Table 2. Results of the identification of the spectrum shown in Fig. 2

The predominance of radiation at transitions of ion spectral lines of nitrogen over the radiation of nitrogen atoms may be due to the recombination mechanism of population of the upper energy levels of atomic nitrogen ions in an overvoltage nanosecond discharge [13]. The energies of the upper energy levels for the spectral lines of N II are in the range of 21–26 eV, which indicates a high temperature of electrons in the studied plasma, since for the passage of recombination of ions with plasma electrons, it is necessary to have doubly charged atomic nitrogen ions.

The recombination mechanism of the formation of excited atoms and ions of the material of electrodes of a microsecond spark discharge in air at atmospheric pressure, using the example of using electrodes made of stainless steel and aluminum, was established in [14]. This conclusion was confirmed in numerous publications on the results of a study of an overvoltage nanosecond discharge between metal electrodes in air and nitrogen ($p = 101$ kPa), summarized in the review [15]. However, photographic recording of plasma emission spectra was used here, and in most cases data on the relative intensities of spectral lines of the electrode material and lines and bands of buffer gases were absent. Such discharges between zinc electrodes at air or nitrogen pressures $p = 1 - 20$ kPa have been poorly studied. The results of studying the spectral characteristics of an overvoltage nanosecond discharge in air ($p = 101$ kPa) between copper electrodes obtained using modern photoelectric recording of spectral characteristics of plasma radiation are given in [16].

The optical and gas-dynamic properties of the cathode spot for a nanosecond discharge in argon are given in [17]. In these studies, radiation was observed from the plasma of the cathode spot with a diameter of $\approx 0.2 - 0.3$ mm and from the plasma of a diffuse discharge, which occupied most of the discharge gap. The main part of the energy of a nanosecond discharge is first introduced into the cathode spot (in the plasma phase); therefore, in the plasma bunch, energy at the initial stage is spent on plasma electrons, and then is transferred to ions. On this basis, the mechanism of formation of excited zinc ions in our experiments is most likely determined by the processes of electron excitation of zinc ions in the main energy field. The effective cross sections for the excitation of zinc ions from the ground energy level are large and reach $10^{-16}$ cm$^2$ [18]. A prerequisite for the occurrence of such processes is a high concentration of electrons in the plasma of overvoltage discharges of nanosecond duration, reaching $10^{17}$ cm$^{-3}$ [19].

## IV. CONCLUSIONS

Thus, it was found that at nitrogen and air pressures in the range of 13–20 kPa between zinc electrodes, at an interelectrode distance of 2 mm, a spatially uniform overvoltage nanosecond discharge with a pulsed electric power of up to 0.7 MW and an energy contribution to the plasma in one pulse was equal to 40 mJ.

The study of the spectral characteristics of plasma based on gas–vapor mixtures "nitrogen–zinc", "air–zinc" showed that in the bactericidal part of the spectrum the most intense were the spectral lines of atoms and singly charged zinc ions, and in the wavelength range 280–400 nm — nitrogen ions and molecules.

The intensity of the spectral lines of Zn I and Zn II increased about two times in the transition from a discharge in a mixture based on air to a discharge in a mixture based on nitrogen, which may be due to the quenching of their upper excited levels by oxygen molecules, which led, presumably, to the formation of molecules, clusters and zinc oxide nanoparticles. The character of the change in the intensity of the spectral

bands of the nitrogen molecule upon going from a nitrogen-based mixture to an air-based mixture indicates that the $C^3\Pi_u^+$ level of the $N_2$ molecule is populated by direct electron impact.

The most probable processes for the formation of excited zinc atoms and ions, as well as nitrogen ions and molecules, can be electron excitation reactions and dielectronic recombination processes. Automatic irradiation of the substrate and film nuclei on the substrate with intense UV radiation of zinc atoms and ions from a nanosecond discharge plasma is promising for influencing the electrical characteristics of synthesized films based on zinc, as well as zinc oxide and nitride.


[1] A. K. Shuaibov, A. A. Malinina, A. N. Malinin, *Overstressed Nanosecond Discharge: in gases at atmospheric pressure and its application for the synthesis of nanostructures based on transition metals* (LAP Lambert Academic Publishing, Beau Bassin, Mauritius, 2021).

[2] V. F. Tarasenko, *Runaway Electrons Preionized Diffuse Discharge* (Nova Science Publishers Inc., New York, 2014).

[3] E. Kh. Bakst, V. F. Tarasenko, Yu. V. Shut'ko, M. V. Erofeev, Quantum Elec. (Woodbury) **42**, 153 (2012); https://doi.org/10.1070/QE2012v042n02ABEH014795.

[4] A. K. Shuaibov *et al.*, Surf. Eng. Appl. Electrochem. **56**, 510 (2020); https://doi.org/10.3103/S106837552004016X.

[5] G. Palani, K. Kannan, D. Radhika, P. Vijayakumar, K. Pakiyaraj, Phys. Chem. Solid State **21** 571 (2020); https://doi.org/10.15330/pcss.21.4.571-583.

[6] G. A. Mesyats, Phys.-Usp. **38**, 567 (1995); https://doi.org/10.1070/PU1995v038n06ABEH000089.

[7] D. V. Beloplotov, A. A. Grishkov, D. A. Sorokin, V. A Shklyaev, Russ. Phys. J. **64**, 340 (2021); https://doi.org/10.1007/s11182-021-02334-1.

[8] A. H. Abduev, A. Sh. Asvarov, A. K. Ahmetov, R. M. Emirov, V. V. Belyaev, Appl. Phys. Lett. **43**, 40 (2017); https://doi.org/10.21883/PJTF.2017.22.45259.16874.

[9] O. K. Shuaibov *et al.*, Ukr. J. Phys. **63**, 790 (2018); https://doi.org/10.15407/ujpe63.9.790.

[10] A. R. Striganov, *Tablitsy spektralnykh liniy neytralnykh i ionizirovannykh atomov* (Atomizdat, Moscow, 1966).

[11] NIST Atomic Spectra Database Lines Form, https://physics.nist.gov/PhysRefData/ASD/lines_form.html.

[12] S. I. Maksimov, A. V. Kretinina, N. S Fomina, L. N. Gall, Nauchnoe priborostroenie **25**, 36 (2015).

[13] D. Z. Pai, D. L. Lacoste, C. O. Laux, Plasma Sources Sci. Technol. **19**, 065015 (2010); https://doi.org/10.1088/0963-0252/19/6/065015.

[14] J. P. Walters, H. V Malmstadt, Anal. Chem. **37**, 1484 (1965). https://doi.org/10.1021/ac60231a010.

[15] L. P. Babich, T. V. Loyko, V. A. Tsukerman, Usp. Fiz. Nauk **160**, 49 (1990); https://doi.org/10.3367/UFNr.0160.199007b.0049.

[16] A. K. Shuaibov, G. E. Laslov, Ya. Ya. Kozak, Opt. Spectrosc. **116**, 552 (2014); https://doi.org/10.1134/S0030400X14030199.

[17] R. Shyker, Y. Binur, A. Szöke, Phys. Rev. A **12**, 512 (1975); https://doi.org/10.1103/PhysRevA.12.515.

[18] A. N. Gomonai, J. Appl. Spectrosc. **82**, 13 (2015); https://doi.org/10.1007/s10812-015-0057-4.

[19] D. Levko, L. L. Raja, Phys. Plasmas **22**, 123518 (2016); https://doi.org/10.1063/1.4939022.


## СПЕКТРОСКОПІЧНА ДІАГНОСТИКА ПЛАЗМИ ПЕРЕНАПРУЖЕНОГО НАНОСЕКУНДНОГО РОЗРЯДУ МІЖ ЕЛЕКТРОДАМИ З ЦИНКУ В ПОВІТРІ Й АЗОТІ


О. К. Шуаібов, Р. В. Грицак, О. Й. Миня, А. О. Малініна, Ю. Ю. Білак, З. Т. Гомокі

*ДВНЗ "Ужгородський національний університет", пл. Народна 3, Ужгород, Україна*



Наведено спектри випромінювання перенапруженого наносекундного розряду між електродами з цинку в повітрі й азоті за тисків 13,3 кПа і 20 кПа відповідно. У процесі мікровибухів неоднорідностей на робочих поверхнях цинкових електродів у сильному електричному полі в розрядний проміжок під час формування ектонів вносяться пари цинку. Це створює передумови для утворення молекул і кластерів цинку, оксиду та нітриду цинку в плазмі й синтезу тонких наноструктурованих плівок цинку, оксиду й нітриду цинку, які можуть осаджуватись на скляній чи кварцовій підкладці, установленій поблизу від центру розрядного проміжку.

Досліджено осцилограми напруги і струму, які мали форму затухаючих у часі осциляцій тривалістю близько 7–10 нс, що зумовлено неузгодженістю вихідного опору високовольтного модулятора з опором навантаження. Установлено, що повна тривалість осциляцій напруги на проміжку та розрядного струму досягала 400-450 нс за тривалості окремих осциляцій напруги 7–10 нс, а осциляції струму мали тривалість $\approx 70$ нс. Величина імпульсної потужності розряду досягала (0.5–0.7) МВт.

Спектральні характеристики розряду досліджували з центральної частини розрядного проміжку величиною 2 мм. Випромінювання плазми реєстрували в спектральному діапазоні $\lambda = 196 - 663$ нм. Установлено основні збуджені складники плазми паро-газових сумішей на основі пари цинку й повітря та азоту, які під час осадження за межами розрядної плазми можуть спричиняти утворення тонких наноструктурованих плівок цинку, нітриду й оксиду цинку. Спектри випромінювання плазми на основі повітря, азоту й пари цинку включали випромінювання атомів й однозарядних йонів цинку та азоту, спектральних смуг другої додатної системи молекули азоту та неперервного випромінювання в спектральній ділянці 210–640 нм.

**Ключові слова:** перенапружений наносекундний розряд, цинк, повітря, плазма.